Original Paper

Journal of Biomedical Science

J Biomed Sci 2003;10:87–97
DOI: 10.1159/000068083

Received: May 25, 2002
Accepted: July 31, 2002

Characterization of Reduced Expression of Glycine N-Methyltransferase in Cancerous Hepatic Tissues Using Two Newly Developed Monoclonal Antibodies

Hsiao-Han Liu[a, b] Kuan-Hsuan Chen[b] Yi-Ping Shih[b] Wing-Yiu Lui[d]
Fen-Hwa Wong[b] Yi-Ming A. Chen[a, b, c]

[a]Institute of Microbiology and Immunology, School of Life Sciences, [b]Division of Preventive Medicine, Institute of Public Health, School of Medicine, [c]AIDS Prevention and Research Center, [d]Department of Surgery, School of Medicine, National Yang-Ming University, Taipei, Taiwan, ROC

Key Words
Glycine N-methyltransferase · Recombinant protein · Monoclonal antibody · Epitope mapping · Hepatocellular carcinoma

Abstract
Glycine N-methyltransferase (GNMT) is a protein with multiple functions. Recently, two Italian siblings who had hepatomegaly and chronic elevation of serum transaminases were diagnosed to have GNMT deficiency caused by inherited compound heterozygosity of the *GNMT* gene with missence mutations. To evaluate the expression of GNMT in cell lines and tissues from hepatocellular carcinoma (HCC) patients, we produced two monoclonal antibodies (mAbs) 4-17 and 14-1 using two recombinant GNMT fusion proteins. M13 phage peptide display showed that the reactive epitopes of mAbs 4-17 and 14-1 were amino acid residues 11–15 and 272–276 of human GNMT, respectively. The dissociation constants of the binding between GNMT and mAbs were 1.7 $\times$ 10^{-8} *M* for mAb 4-17 and 1.8 $\times$ 10^{-9} *M* for mAb 14-1. Both mAbs can identify GNMT present in normal human and mouse liver tissues using Western blotting (WB) and immunohistochemical staining assay (IHC). In addition, WB with both mAbs showed that none of 2 hepatoblastoma and 5 HCC cell lines expressed GNMT. IHC demonstrated that 50% (13/26) of nontumorous liver tissues and 96% (24/25) of HCC tissues did not express GNMT. Therefore, the expression of GNMT was downregulated in human HCC.

Introduction

Glycine N-methyltransferase (GNMT, EC 2.1.1.20) was found originally as an enzyme regulating the ratio of S-adenosylmethionine (SAM) to S-adenosyl- homocysteine by catalyzing the synthesis of sarcosine from glycine and SAM [23, 32]. GNMT is conservative among different animal species [5, 9, 26, 33]. In halophilic Methanoarchaea, GNMT plays a major role in osmoregulation [25]. In rabbit and rat livers, GNMT comprises 1–3% of the cytosolic proteins, and the enzyme was suggested to play an important role in the metabolism of methionine [13, 20, 32].

Previously, through mRNA differential display and Northern blot analysis of tumor and nontumorous liver tissues from human hepatocellular carcinoma (HCC) patients, we reported that the expression level of GNMT was diminished in tumorous tissues and HCC cell lines [9]. Subsequently, the human *GNMT* gene was isolated, sequenced and mapped to chromosome 6p12 [10]. Fur-

KARGER
Fax + 41 61 306 12 34
E-Mail karger@karger.ch
www.karger.com

1021–7770/03/0101–0087$19.50/0
Accessible online at:
www.karger.com/jbs

Prof. Yi-Ming A. Chen
Institute of Public Health, National Yang-Ming University
Taipei 112, Taiwan (ROC)
Tel. +886 2 28267304, Fax +886 2 28270576
E-Mail arthur@ym.edu.tw

thermore, genotypic analyses of different polymorphisms of the human *GNMT* gene demonstrated that 36–47% of the genetic markers showed loss of heterozygosity in the tumorous tissues of HCC patients [37]. Functional characterization of GNMT showed that GNMT is able to bind benzo[a]pyrene (BaP) and decrease BaP-DNA adduct formation [4, 7, 21, 35]. Therefore, *GNMT* can be classified as a tumor susceptibility gene.

Recently, Mudd et al. [30] reported that two Italian siblings who had mild hepatomegaly and chronic elevation of serum transaminases were diagnosed to have GNMT deficiency. Both children were compound heterozygotes for the *GNMT* gene with missense mutations [27]. In this report, we used two different protein expression systems to produce GNMT fusion proteins and generate monoclonal antibodies (mAbs). Two mAbs against GNMT were obtained and further characterized. Through Western blot and immunohistochemical staining assays with both mAbs, the expression of GNMT was found to be downregulated in human HCC cell lines and tissues.

Methods

Construction of the pGEX-GNMT and pGNMT-His Plasmids (fig. 1)

For the construction of the pGEX-GNMT, a full-length GNMT cDNA fragment was cleaved from pBluescript-GNMT-9-1-2 phagemid DNA [9] by using *Sma*I and *Sal*I restriction enzymes (Stratagene, La Jolla, Calif., USA). This 1.2-kb DNA fragment was ligated to a vector, pGEX-KG [19] that had previously been digested with *Sma*I and *Xho*I.

In terms of the construction of pGNMT-His, as shown in figure 1b, plasmid pCMV-GNMT [7] was used as a template in the polymerase chain reaction (PCR). A 1.2-kb DNA fragment containing the GNMT cDNA sequence and restriction enzyme sites on both ends was amplified. Twenty PCR cycles were performed in a DNA Thermal Cycler (Perkin Elmer Cetus, Foster City, Calif., USA) using their Amplitaq Gold Taq DNA polymerase. The upstream primer (5′-GAGGAATTCATGGTGGACAGCGTGTAC) consisted of a 3-bp 'clamp' (GCG) at the 5′ end, followed by one restriction enzyme site (*Eco*RI) and a GNMT cDNA sequence. The downstream primer (5′-GCGCTCGAGGTCTGTCCTCTTGAGCAC) contained a similar structural sequence motif as the upstream primer, except that it consisted of negative strand sequences from the terminal region of GNMT cDNA and a different restriction enzyme site (*Xho*I). After the PCR, the 1.2-kb DNA fragment was gel purified, digested with *Eco*RI and *Xho*I and ligated to a vector pET29a (Novagen, Inc., Madison, Wisc., USA), which had been digested with the same pair of restriction enzymes. The DNA sequences of the both plasmids were confirmed by automated DNA sequencing with ABI Prism dye terminator cycle sequencing core kit (Perkin-Elmer Cetus).

Escherichia coli strain JM109 or BL21 was used as the recipient in the transformation and expression experiments for pGST-GNMT. In addition, plasmid pGEX-KG [19] was used for the induction and purification of glutathione S-transferase (GST) protein, which served as a parallel control in the enzyme immunoassay.

Expression and Purification of Different GNMT Recombinant Proteins

All the GST, GST-GNMT and GNMT-His recombinant proteins (RPs) were induced in JM109 or BL21 cells using isopropyl-beta-*D*-thiogalactopyranoside (IPTG). Both the GST and GST-GNMT RPs were purified using glutathione-Sepharose 4B beads (Pharmacia, Uppsala, Sweden) as described by Guan et al. [19]. The GNMT-His RP was purified using an Ni^{2+}-charged histidine (His)-binding resin column according to the procedures provided by the manufacturer (Novagen). The bound GST-GNMT-RP was eluted from the glutathione-Sepharose 4B beads using a 5 m*M* reduced glutathione buffer. The thrombin digestion method was used to purify GNMT RP from the bead-bound GST-GNMT fusion protein. The concentrations of the RPs were measured using Pierce BCA protein assay reagent (Pierce, Rockford, Ill., USA) and the purity was analyzed by running the samples on a 12.5% SDS-polyacrylamide mini-gel (Bio-Rad Laboratories, Richmond, Calif., USA).

Production of a Rabbit Anti-GNMT Antiserum

To raise rabbit antibodies against GNMT, purified GST-GNMT RP was mixed with Freund's complete (for the initial immunization) or incomplete (for the booster injections) adjuvant (Sigma Co., St. Louis, Mo., USA) and the resultant mixture was used as an immunogen to inoculate 8-week-old NZW rabbits (150–200 μg RP per rabbit) subcutaneously. Rabbits received booster injections every 3 weeks after the initial injection with additional doses of the same RP. Rabbit sera were collected before the immunization and 1 week after each injection. All sera were heat inactivated at 56°C for 30 min and stored at –20°C.

Preparation of mAbs against GNMT

Murine mAbs were produced by the hybridoma technique commonly used in our laboratory. Briefly, BALB/c mice were immunized with purified GST-GNMT and GNMT-His RPs mixed with complete (for primary immunization) or incomplete (for booster injections) Freund's adjuvant (Sigma), at 10-day intervals by intraperitoneal injection with dosage about 25 μg of RP per inoculum. Serum samples were collected from the tail vein before the immunization and 1 week after each injection. Three days after the last intravenous injection of RP, fusion of the splenocytes of immunized mice with mouse myeloma cells NS1 (American Type Culture Collection, Rockville, Md., USA) was performed with PEG1500 (Roche Diagnostics GmbH, Mannheim, Germany), and cultured on ninety-six-well plates [12]. The culture supernatants were screened using the GST/GNMT EIA and with WB strips blotted with GST, GST-GNMT, GNMT-His RP. Selected hybridoma cells were expanded and cloned at least twice by limiting dilution and grown as ascitic tumors in BALB/c mice primed with 0.5 ml pristine (Sigma). mAbs were purified and concentrated in Protein-A antibody purification kits (Pro-Chem Inc. Acton, Mass., USA.) and Centricon Plus-80 columns (Millipore, Bedford, Mass., USA).

Cell Lines and Culture

Two human hepatoblastoma cell lines-HepG2 [1, 22], Huh 6 [31], and five HCC lines-Huh 7 [31], HA22T [6], PLC/PRF/5 [28], Hep3B and Sk-Hep1 [1, 15,16] were used in this study. These cells were cul-

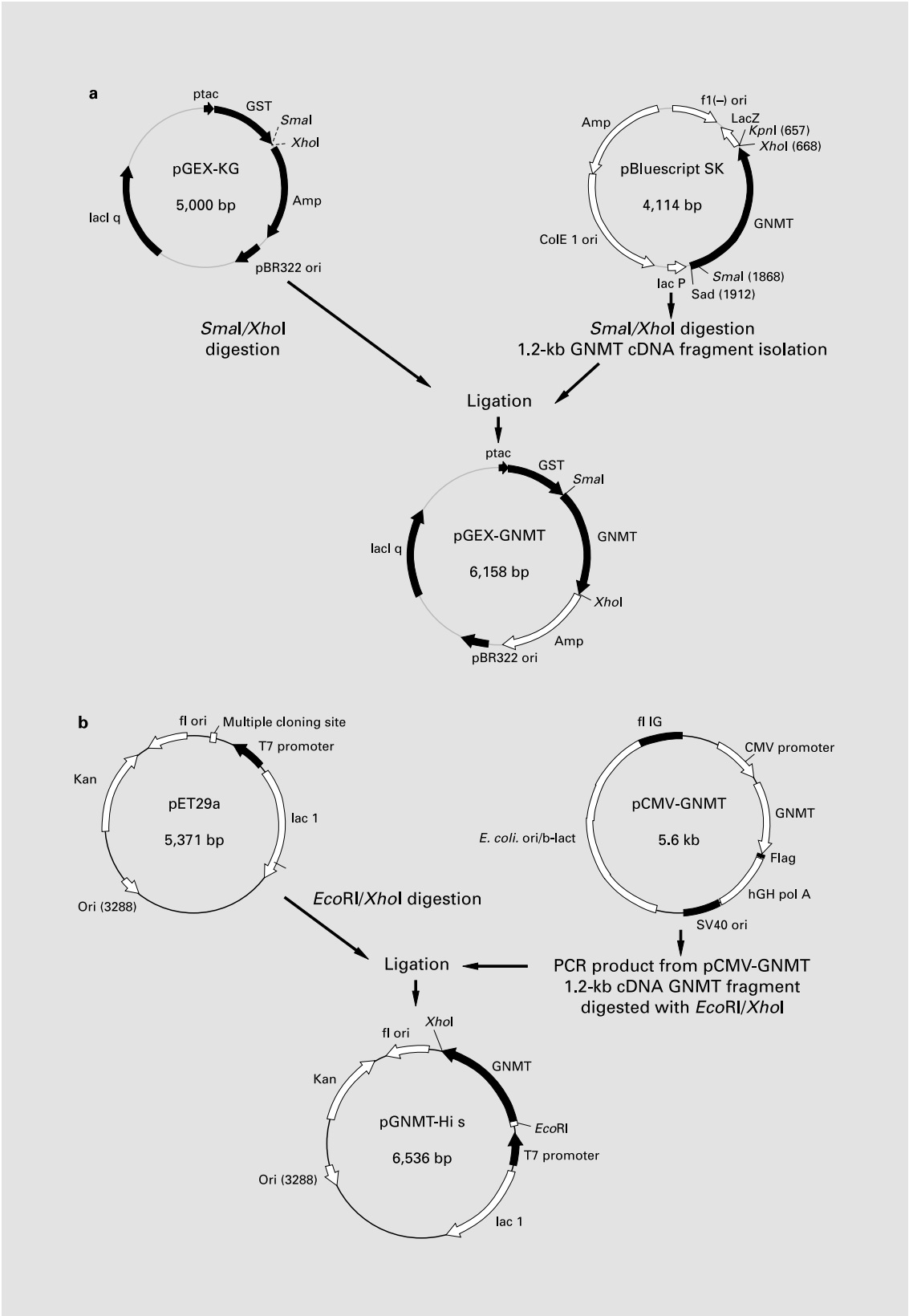

Fig. 1. Construction of two recombinant GNMT expression plasmids pGEX-GNMT (a) and pGNMT-His (b).

tured in Dulbecco's modified Eagle's medium (Gibco BRL, Grand Island, N.Y., USA) with 10% heat-inactivated fetal bovine serum (HyClone, Logan, Utah), penicillin (100 U/ml), streptomycin (100 μg/ml), nonessential amino acids (0.1 m*M*), fungizone (2.5 mg/ml), and *L*-glutamine (2 m*M*) in a humidified incubator with 5% CO_2. Hygromycin (20 μg/ml) was added to the SCG2-1-4 cells were added for maintenance of the expression of GNMT cDNA.

The NS 1 cells were cultured in RPMI-1640 medium (Gibco) supplemented with 10% heat-inactivated fetal calf serum, 2 m*M* *L*-glutamine, penicillin (100 IU/ml) and streptomycin (100 IU/ml) as described in Chu et al. [12].

Enzyme Immunoassay

EIA was used to monitor the antibody titers of the immunized animals and to screen for mAbs in the supernatant of different hybridomas. Ninety-six-well plate coated with either GST-GNMT or GNMT-His RP at a concentration of 1 μg/ml (100 μl per well) was used. The antibody titers of either rabbit or mouse serum were determined at a serial 10-fold dilution. To screen the hybridomas from animals immunized with GST-GNMT RP, enzyme immunoassay (EIA) plates coated with GST were also used to rule out those mAbs reactive with the GST. Additionally, to screen the hybridomas from animals immunized with GNMT-His RP, GST-GNMT-coated plates were used to confirm those positive clones screened by the GNMT-His-coated plates. A rabbit anti-GNMT antiserum (R4) and several mouse anti-GNMT anti-sera were used as the positive controls in the EIA. Details of the procedures have been described previously [11].

The concentrations of mAbs were determined by mouse IgG EIA quantitation kits (Bethyl Laboratory, Montgomery, Tex., USA) and the immunoglobulin concentrations were analyzed using EIA ElX808 readers with 4-parameter logistic regression (Bio-Tek Instruments, Winooski, Vt., USA). All the isotyping and light chain determinations were done using mouse immunoglobulin isotyping ELISA kits (BD Biosciences Pharmingen, San Diego, Calif., USA).

Western Blot Assay and Radioimmunoprecipitation

Both WB and RIP were used for the confirmation of the mAbs against GNMT. Three RPs – GST-GNMT (58 kD in size), His-GNMT (37.4 kD in size), GST (26 kD in size) – human and mouse liver proteins were used as the antigens in the Western blot (WB). After incubation of mAbs 14-1, 4-17, anti-β-actin mAb (Sigma) and normal mouse serum, washed the strip or nitrocellulose membrane, and reacted with horseradish-peroxidase-conjugated goat antimurine immunoglobulin (Sigma), and finally developed with 3,3′-diaminobenzidine tetrahydrochloride solution (Zymed Laboratories Inc. Calif., USA (GST, GST-GNMT, GNMT-His RP) or ECL reagent (Amersham) as described previously [8]. Radioimmunoprecipitation (RIP) was used as an alternative method to confirm the mAbs. [^{35}S]-cysteine and [^{35}S]-methionine (New England Nuclear, Boston, Mass., USA)-labeled SCG2-1-1 cells were used as antigens in the RIP [7]. A rabbit anti-GNMT antiserum (R4) was used as the positive control in the assays. The procedures of the WB and RIP were described previously [11].

Epitope Mapping with M13 Phage Peptide Display

The antibodies were diluted with 0.1 *M* $NaHCO_3$ (pH 8.6) to a concentration of 100 μg/ml, and added to 5-ml sterile polystyrene petri dishes. After coating overnight at 4°C in a humidified container, the plates were blocked with the blocking buffer (0.1 *M* $NaHCO_3$ pH 8.6, 5 mg/ml BSA, 0.02% NaN_3, with a sterilized filter, stored at 4°C) and incubated for at least 1 h at 4°C. M13 phages displaying random heptapeptides at the N-terminus of their minor coat protein (pIII) were used (Ph.D.-7TM Phage Display Peptide Library, New England Biolabs Inc. Beverly, Mass., USA). Specifically bound phages were selected according to the manufacturer's instructions. The 5′-end nucleotides of gene III from the picked phages were sequenced and then encoded peptides were deduced [14].

Coupling of GNMT to the Biosensor Surface

A carboxymethyl dextran (CMD) sample cuvette was purchased from Thermo Labsystems. In initial experiments, the coating conditions were optimized with regard to the pH. The surface was equilibrated in 10 m*M* sodium acetate buffers, with pH ranging from 4 to 6 in 0.5-unit steps for 6 min. Samples of 9 μg human GNMT RP (thrombin-cleaved) in the same buffer were then added to the cuvette. To test, optimized pH conditions were created. The binding of the RP to the cuvette, which is due to electrostatic attraction between the negatively charged carboxyl groups on the dextran and the positively charged protein, was performed for 6 min. The optimized response occurred at pH 5.0 in a 10 m*M* acetate buffer. Nine micrograms of GNMT RP cleaved by thrombin were used to couple the CMD surface cuvette in 10 m*M* sodium acetate buffer under optimized pH by the 1-ethyl-3-(3-dimethylaminopropyl) carbodiimide (EDC)/N-hydroxysuccinimide (NHS) method as described previously [18].

Determination of the Dissociation Constants of mAbs Using an IAsys Affinity Sensor

Following the immobilization of GNMT, a PBST/Tween 20 (PBST) baseline was established, and the stirred rate in the cuvette was kept constant at 100 rpm for all reactions. A series of 2-fold dilutions (in 200 μl PBST) of mAb from culture supernatant were added to the cuvette, and the responses were measured by IAsys control software 3.01. Kinetic analysis of the binding data was undertaken using the curve-fitting kinetic analysis software FAST fit (Thermo Labsystems, Affinity Sensors Division, Cambridge, UK) designed for the IAsys, and K_d, determined as previously described [29].

Immunohistochemistry by Antibodies against GNMT

Two sets of tumor and nontumorous liver tissues from HCC patients were used for the immunohistochemical procedures with mAbs and R4. The first set included 13 nontumorous and 9 tumor tissues (7 pairs) and the second set included 13 nontumorous and 16 tumor tissues (9 pairs). All the cancerous and noncancerous tissue specimens were confirmed by pathologic examination. The study was approved by the institutional review board of the Taipei Veterans General Hospital (IRB No.: 90-02-01A). The tissue blocks fixed in paraffin were sliced into 6-μm-thick sections, deparaffinized and immersed in a 3% solution of hydrogen peroxide in distilled water for 5 min to abolish the endogenous peroxidase reaction. Primary antibodies, mAb 14-1 (1:100 dilution of the ascites) or mAb 4-17 (1:25 dilution of the ascites) or R4 (1:200 dilution), were applied to the tissues. A ready-to-use biotinylated secondary antibody was applied to bind the primary antibody. A streptavidin-peroxidase conjugate is applied to the same tissue slide (HistoST5050 detection kit, Zymed Laboratories Inc.). The presence of peroxidase is revealed by addition of 3,3′-diaminobenzidine tetrahydrochloride solution for color reaction as described in Chen et al. [9].

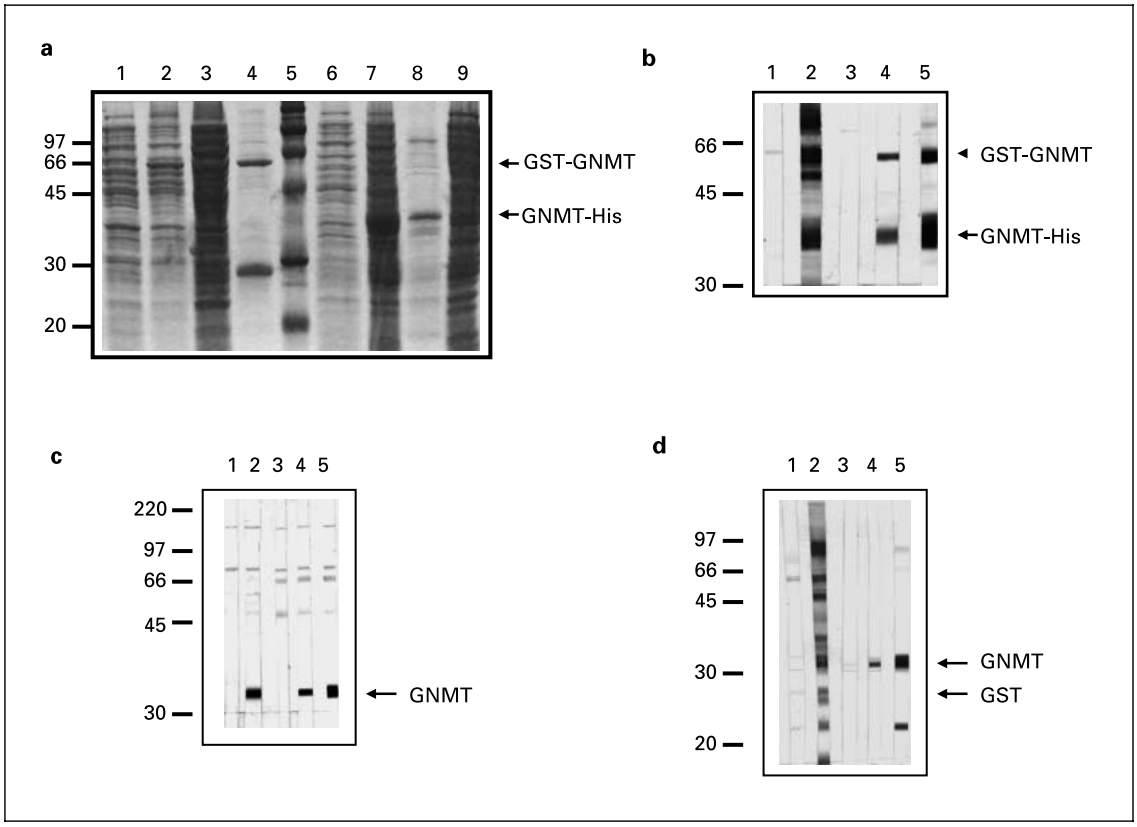

Fig. 2. Identification of recombinant and native forms of GNMT with mAbs 14-1 and 4-17. a Coomassie Brilliant Blue R250 staining of a SDS-polyacrylamide gel containing lysates from *E. coli* (JM109) harboring pGEX-GNMT, or (BL21) harboring pGNMT-His before (lanes 1, 6) and after (lanes 2, 7) IPTG induction. The unbound (lanes 3, 9) and the eluent of the bound fractions (lanes 4, 8) from the glutathione agarose bead and nickel affinity column for the His tag purification procedure were also run in lanes 4 and 8, respectively. b WB of mAbs to strips with GST-GNMT and GNMT-His recombinant proteins. Strips were reactive with a preimmunized rabbit serum (lane 1), a rabbit anti-GST-GNMT antiserum-R4 (lane 2), a normal mouse serum (lane 3), mAb 14-1 (lane 4) and mAb 4-17 (lane 5). These strips used the indirect method, and exhibited color by substrate 3,3′ diaminobenzidine. c WB assays on strips with cell lysates from 293T cells transfected with pCMV-GNMT plasmid DNA. d WB assays on strips with GST and GNMT. Antibodies used in c, d: lane 1, preimmunized rabbit serum; lane 2, R4; lane 3, normal mouse serum; lane 4, mAb 4-17; and lane 5, mAb 14-1. Molecular weight markers were labeled at the left margin (in kD) of each panel except a (lane 5).

Results

Expression and Purification of Two GNMT Recombinant Proteins

Two plasmids (pGEX-GNMT and pGNMT-His) were constructed and confirmed by automated DNA sequencing (data not shown). To induce the fusion protein, *E. coli* BL21 or JM109 cells harboring different plasmids were grown at 37°C in LB broth containing 50 μg/ml ampicillin, and the RPs were induced using IPTG as described in the methods mentioned above [19]. For analysis of the synthesized fusion protein, 10-μl aliquots of both the IPTG-induced and noninduced bacterial pellets, solubilized in sample buffer, were analyzed using electrophoresis on a 12.5% SDS-polyacrylamide gel, and the induced RPs were visualized by staining with Coomassie brilliant blue 250. As shown in figure 2a, GST-GNMT and GNMT-His RPs, with sizes of 57 and 37.4 kD, respectively, appeared in the IPTG-induced bacterial lysates (fig. 2a, lanes 2, 7). Each RP was further purified using glutathione Sepharose-4B beads or His-binding resin (fig. 2a, lanes 4, 8). WB assays with a rabbit anti-GNMT antiserum (R4) were used to identify the RPs (fig. 2b, lane 2). Preimmunized serum from the R4 rabbit was used as a negative control in the WB assay (fig. 2b, lane 1).

Table 1. Epitope mapping of mAbs 14-1 and 4-17 using M13 phage peptide display

a mAb 14-1

GNMT sequence	271 G	**D**	**F**	**K**	**P**	**Y**	**K**	278 **P**
M13 phage display								
1	I	K	T	P	–	W	–	
2		H	–	–	–	H	–	V
3		H	–	–	–	H	–	V
4		H	–	–	–	F	R	L
5		Y	Y	–	–	–	–	–
6		–	Y	–	–	F	R	A
7	W	–	–	–	–	–	R	
8	T	E	–	–	–	–	R	
9		E	–	–	–	F	–	Y
Consensus sequence		X	**F**	**K**	**P**	X	K/R	X

b mAb 4-17

GNMT sequence	9 R	S	**L**	**G**	**V**	**A**	**A**	16 **E**
M13 phage display								
1		A	–	–	T	–	–	F
2		R	W	–	T	–	–	F
3		**T**	W	–	T	–	–	W
4	Q	A	–	–	I	–	–	
5	K	**T**	–	–	Y	–	–	
6		A	M	–	–	–	F	R
Consensus sequence			**L**	G	T	A	A	

Residues which appeared as conservative amino acids are indicated with dash marks. The letter X represents residue without preferred biophysical property.

Generation and Characterization of mAbs against GNMT

The purified GST-GNMT and GNMT-His RPs were used as the antigens for generation of mAbs against GNMT. In total, 3 different fusion and screening experiments were performed. Two mAbs were eventually generated. mAb 14-1 was produced by using the GST-GNMT as the antigen, while mAb 4-17 was generated by using the GNMT-His as the antigen in the immunization process. Both mAbs 14-1 and 4-17 reacted with GST-GNMT and GNMT-His RPs (fig. 2b, lanes 4, 5). In addition, they can identify a protein with 32 kD in size in 293T cells transfected with pCMV-GNMT plasmid DNA (fig. 2c, lanes 4, 5). This protein, presumably GNMT, can also be recognized by a rabbit anti-GNMT antiserum-R4 (fig. 2c, lane 2). To rule out the possibility that both mAbs recognize the GST tag fused to the GST-GNMT RP, the GST-GNMT RP was cleaved with thrombin and used as antigens in WB. The results showed that although R4 can recognize the GST protein, both mAbs 4-17 and 14-1 only reacted to the GNMT RP (fig. 2d).

The isotypes and light chain of the mAb were determined using mouse immunoglobulin isotyping EIA kits. The subclasses of mAbs 14-1 and 4-17 were IgG2a and IgG1, respectively, and both mAbs had kappa chains (data not shown).

Epitope Mapping of mAbs 14-1 and 4-17

The epitopes that could be recognized by mAbs 14-1 and 4-17 were mapped using a peptide library displayed on M13 phages. After 3 biopannings, 9 and 6 reactive phage colonies were isolated for mAbs 14-1 and 4-17, respectively. As shown in table 1, the heptapeptides displayed at the N-terminus of the phage pIII protein were deduced by sequencing. More than half of isolated phages displayed a major sequence (consensus sequence) that

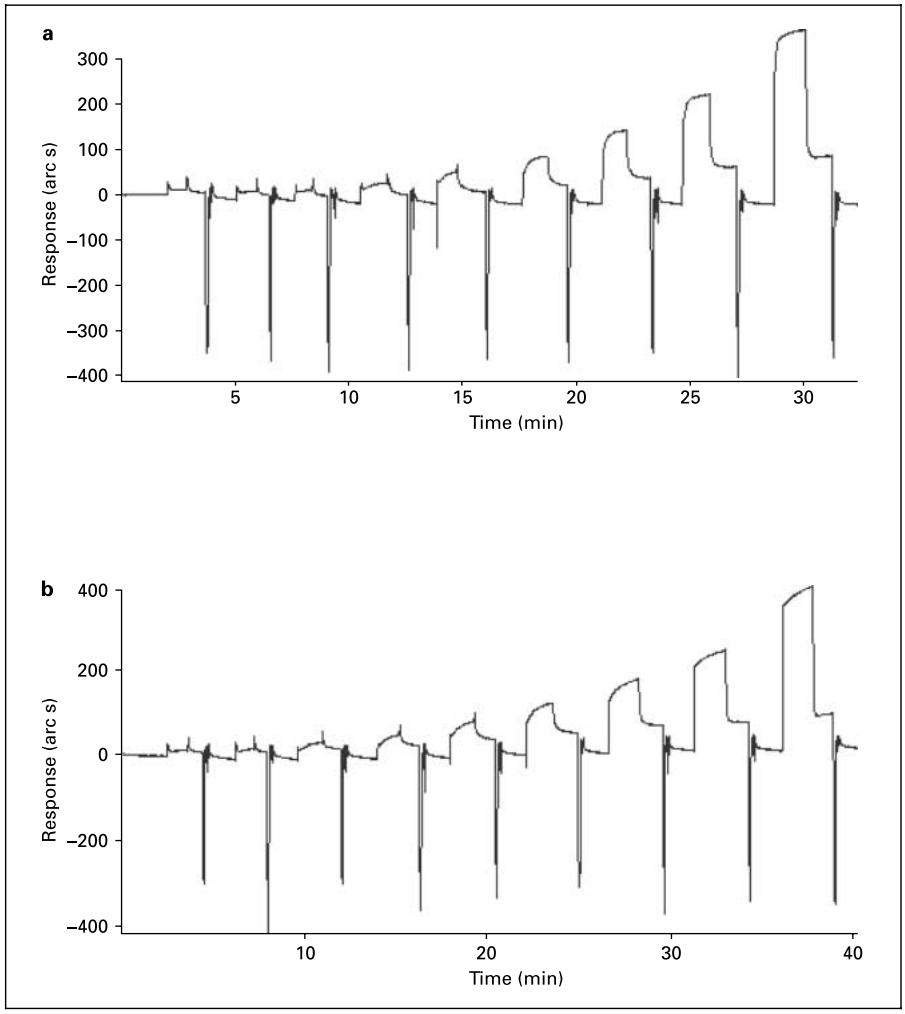

Fig. 3. Response plots of mAbs 14-1 and 14-7 to a cuvette coupled with recombinant GNMT. A two-fold dilution in PBST of 200 µl of culture supernatant was added to the cuvette, and the response was measured by IAsys control software version 3.01. The resulting dissociation constant of these two mAbs was calculated by FAST fit. a Immunoglobulin concentration of mAb 14-1: (1) 4×10^{-11}, (2) 8×10^{-11}, (3) 1.6×10^{-10}, (4) 3.2×10^{-10}, (5) 6.3×10^{-10}, (6) 1.3×10^{-9}, (7) 2.5×10^{-9}, (8) 5.1×10^{-9}, (9) 1.0×10^{-8} *M*. b Immunoglobulin concentration of mAb 4-17: (1). 4.7×10^{-11}, (2) 9.4×10^{-11}, (3) 1.9×10^{-10}, (4) 3.8×10^{-10}, (5) 7.5×10^{-10}, (6) 1.5×10^{-9}, (7) 3×10^{-9}, (8) 6×10^{-9}, (9) 1.2×10^{-8} *M*.

could be used to identify the reactive epitopes for both mAbs. When the consensus sequences were aligned with the human GNMT protein sequence, the best matched regions spanned amino acid residues 272–276 for mAb 14-1 and residues 11–15 for mAb 4-17 (table 1).

The Dissociation Constant of mAbs 14-1 and 4-17

After testing a series of acetate buffers at 0.5 pH intervals per unit, a pH 5 for GNMT was used for the coupling experiment. Recombinant GNMT was coupled to CMD by EDC/NHS in a 10 m*M* acetate buffer at pH 5.0. The affinity of mAbs 14-1 and 4-17 for GNMT was determined by using the affinity sensor with a CMD cuvette. As shown in figure 3, the IAsys response plots demonstrated that there were specific responses of mAbs to GNMT RP coupled in the cuvette (fig. 3a, b). The responses of the mAbs were analyzed using the FAST fit program. The dissociation constants of mAb 14-1 and mAb 4-17 were deduced as 1.8×10^{-9} and 1.7×10^{-8} *M*, respectively.

Expression of GNMT in Different Liver Cancer Cell Lines and Tissues

The expression of GNMT in hepatoma cell lines was examined using WB with both mAbs. The results showed that neither mAb 14-1 nor mAb 4-17 detected GNMT in 2 hepatoblastoma cell lines (HepG2 and Huh-6) and 5 HCC cell lines (Huh 7, HA22T, Hep3B, Sk-Hep1 and PLC/PRF/5) (for mAb 4-17; fig. 4a; for mAb 14-1, data not shown). As controls, mAb 4-17 reacted to the GNMT present in the nontumorous liver tissue from an HCC patient and the liver tissue from a C57/BL mouse (fig. 4a, lanes 1, 2). Figure 4b was used to demonstrate the quality and quantity of proteins in the cell lysates from each cell line or tissue.

We further analyzed the expression level of GNMT in the tumor and nontumorous liver tissues from HCC patients using IHC staining with mAb 14-1 and 4-17 and rabbit antiserum R4. As shown in figure 5, GNMT was mainly present in the cytoplasm of the hepatocytes in the periportal region of the liver. In the first set of IHC with mAb 14-1, 38.5% (5/13) of the nontumorous tissues and none of 9 tumorous tissues had GNMT expression; in the second set of IHC with mAb 4-17, 61.5% (8/13) of the nontumorous tissues and 6.3% (1/16) of the tumorous tis-

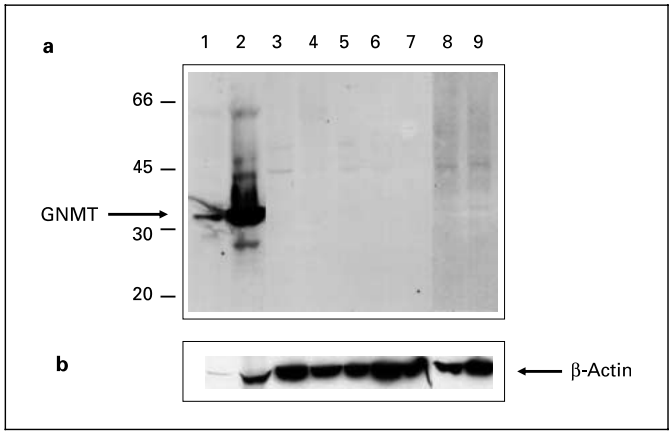

Fig. 4. Western blot analysis of the presence of GNMT in human liver, mouse liver, hepatoblastoma (HepG2 and Huh 6) and hepatocellular carcinoma cell lines (PLC/PRF/5, Huh 7, HA22T, Hep3B and Sk-Hep 1) with mAb 4-17 (a) or anti-β-actin antibody (b). Lane 1, non-tumorous tissue from a hepatoma patient; lane 2, liver from a C57/BL mouse; lane 3, HepG2; lane 4, PLC/PRF/5; lane 5, Huh 6; lane 6, Huh 7; lane 7, HA22T; lane 8, Hep3B; and lane 9, Sk-Hep1. Molecular weight markers were labeled at the left margin (in kD).

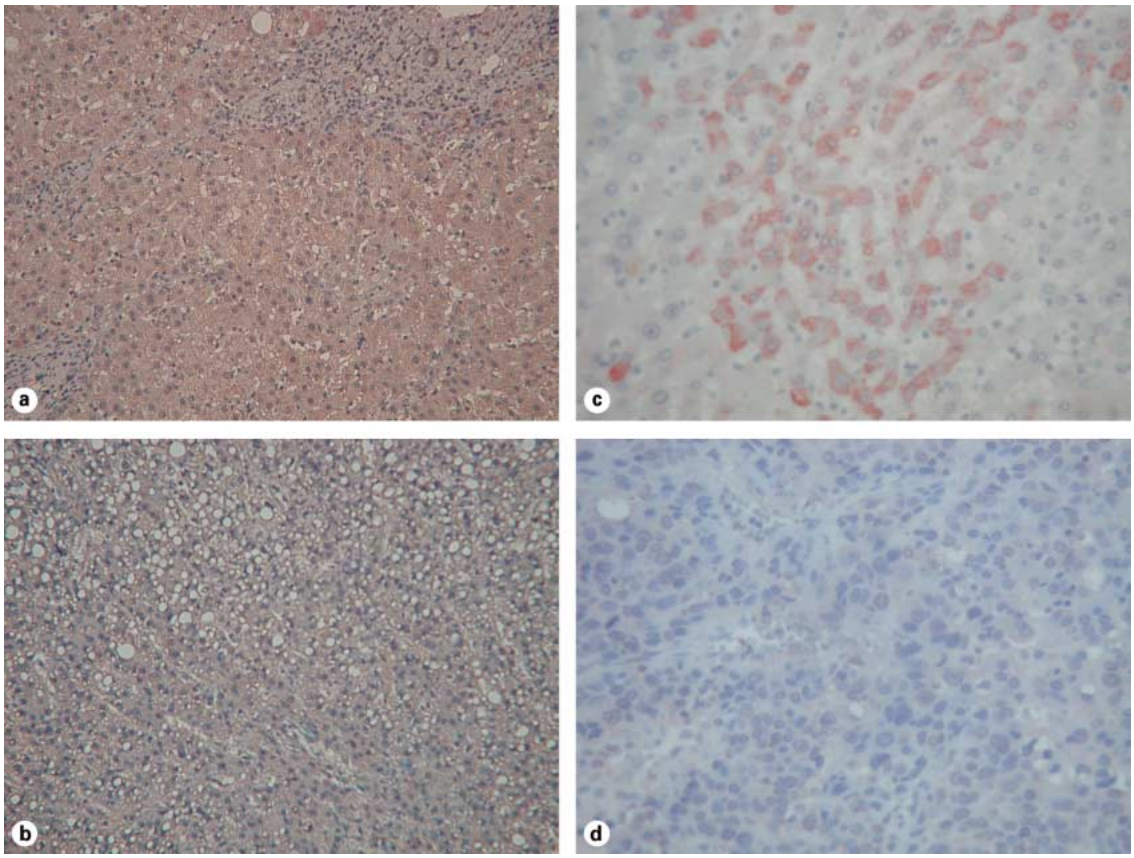

Fig. 5. Immunohistochemical analysis of the GNMT expression using mAb 4-17 or 14-1 in the paraffin-fixed liver tissue sections from two HCC patients. The sections were exposed to mAb 4-17 at 1:25 dilution (a, b) or mAb 14-1 at 1:100 dilution (c, d) and visualized by a labeled streptavidin-biotin method. a (non-tumorous) and b (tumor tissue) were from an HCC patient-H126 (100-fold magnification). c (non-tumorous) and d (tumor tissue) were from another HCC-patient-H146. ×400.

Table 2. The results of the immunohistochemical staining of GNMT in the tumor (T) and non-tumorous (N) tissues from HCC patients

Antibody[a]	Rates of positive staining		Cases among the tissue pairs with different GNMT staining[b]				
	T tissues	N tissues	N+/T+	N+/T–	N–/T+	N–/T–	total pairs
mAb 14-1	0% (0/9)	38.5% (5/13)	0	3	0	4	7
mAb 4-17	6.3% (1/16)	61.5% (8/13)	1	3	0	5	9
Total	4.0% (1/25)	50% (13/26)	1	6	0	9	16

[a] The dilutions for mAbs 14-1 and 4-17 (ascites) were 1:100 and 1:25, respectively.
[b] N+/T+: positive GNMT staining in both the nontumorous and tumor tissues; N+/T-: positive GNMT staining in the nontumorous tissue and negative GNMT staining in the tumorous tissue, etc.

sues had GNMT expression. In total, 50% (13/26) of nontumorous liver tissues and 96% (24/25) of HCC tissues did not express GNMT (table 2). R4 was also used in the second set of IHC and the results showed that 84/6% (11/13) of the nontumorous tissues and 37.5% (6/16) of the tumorous tissue had GNMT expression. In addition, when paired samples (tumor and nontumorous tissues from the same patient) were analyzed, 9 of 16 (56.3%) pairs were found to have an N–/T– staining pattern, 6 of 16 (37.5%) had an N+/T– staining pattern and 1 of 16 (6.3%) had an N+/T+ pattern (table 2).

Discussion

In this study, we have generated and characterized 2 mAbs against GNMT and used them to examine the expression levels of GNMT in HCC cell lines and tissues. Since human GNMT shares 92.2% amino acid sequence homology with murine GNMT protein [2], it is more difficult for GNMT than for other proteins with lower sequence homology with mouse proteins to elicit an antibody response in mice. Initially, we used GNMT cleaved from GST-GNMT fusion protein to raise rabbit anti-GNMT antiserum. It was not successful after we immunized two rabbits more than 5 times. When the antigen was replaced with GST-GNMT fusion protein, high titer rabbit anti-GNMT antisera were obtained in the same rabbits after only another two boosters. The initial failure of the immunization may have been due to the highly conserved amino acid sequences between human and rabbit GNMT [9, 33] or because the cleaved GNMT protein was less stable than the GST-GNMT fusion protein. Furthermore, some epitopes present in the native form of GNMT may be exposed in the fusion protein and may have stimulated antibody responses in animals. Therefore, in the subsequent experiments, it was decided to use either GST or His fusion protein as the antigen to immunize BALB/c mice.

From the epitope mapping data, we found that mAb 14-1 was reactive to the C-terminal amino acid residues 272–276 of GNMT and mAb 4-17 was against an epitope residing at the N-terminus of GNMT (amino acid residues 11–15). According to the X-ray crystallography of rat GNMT, the N-terminal region (amino acid residues 1–23) of GNMT protrudes from the main body of the protein and interacts with other subunits in the central hole of the tetrameric form of GNMT [17, 34]. The C-terminal epitope for mAb 14-1 is in the SAM-binding domain of GNMT [34] (fig. 6). These two regions are conserved in GNMT proteins from humans and the pig, mouse, rat and rabbit. Therefore, these mAbs may be useful for the study of the structure and biological function of GNMT.

The strength of the interactions between mAbs and their reactive antigens can be measured quantitatively. In this study, we used an optical biosensor with a cuvette coupled with recombinant GNMT protein to measure the K_d of mAbs 14-1 and 4-17 to GNMT. The results showed that there were relatively high affinities between the mAbs and GNMT. The affinity of mAb 14-1 was higher than that of mAb 4-17 (the K_d for mAbs 4-17 and 14-1 were 1.7×10^{-8} *M* and 1.8×10^{-9} *M*, respectively). It has been reported that the affinities between antibody and antigen varies enormously, with K_d ranging from 10^{-3} to 10^{-14} *M* [36].

This pair of mAbs was then used to examine the expression levels of GNMT in HCC cell lines and tissues. The results showed that in WB, none of two hepatoblastoma and 5 HCC cell lines expressed GNMT. Since both hepatoblastoma cell lines-HepG2 and Huh-6 have been

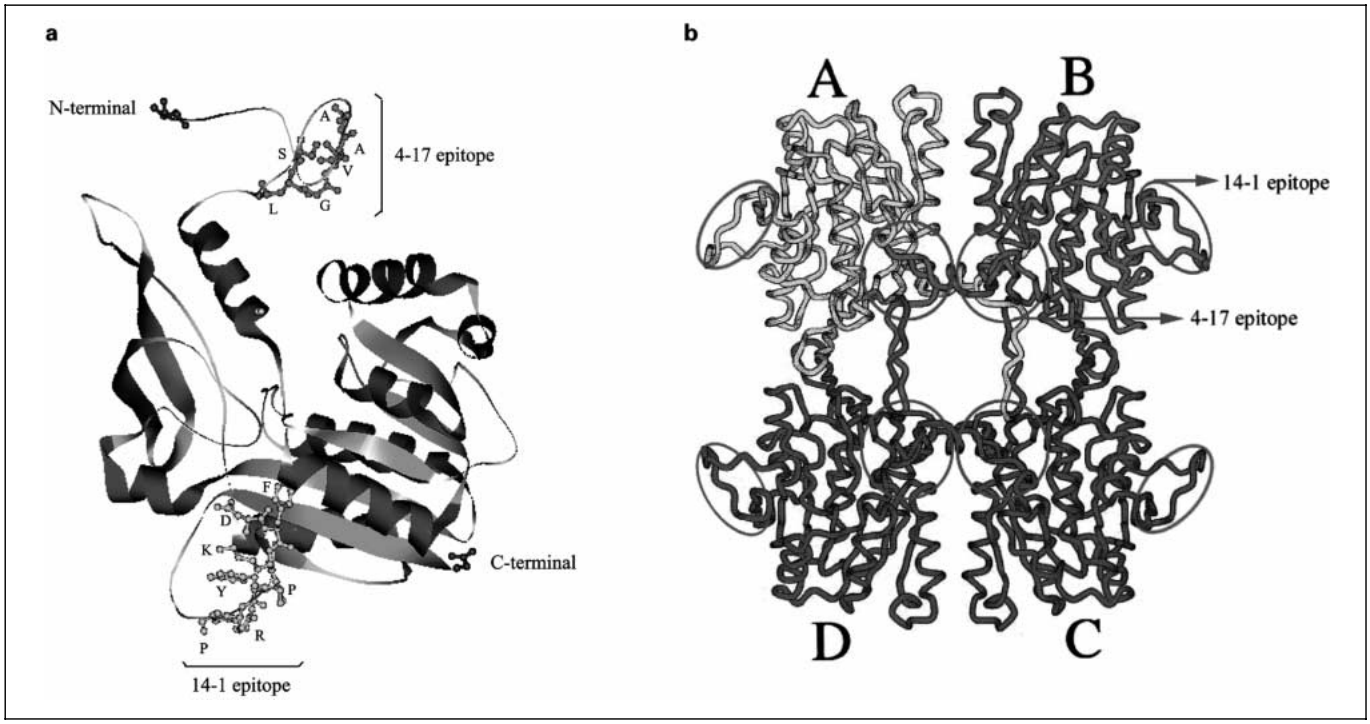

Fig. 6. Locations of the epitopes reactive with mAb 14-1 and 4-17 in the molecular models of rat GNMT. a GNMT in monomeric form. The N-terminal and C-terminal amino acids, as well as the epitope that mAb 14-1 or 4-17 reacted with were displayed in ball and stick model. b GNMT in tetrameric form. The epitope that mAb 14-1 or 4-17 reacted with was indicated by arrows. These models were based on the structures published by Fu et al. [17].

demonstrated to contain decreased levels of GNMT mRNA by Northern blotting [9], the discrepancy may be due to the difference of the sensitivities between these two assays. RT-PCR with specific primers for GNMT cDNA was used to address this issue and the results showed that both HepG2 and Huh-6 cells contained small amounts of GNMT mRNA [unpubl. results].

Due to the advances of early diagnosis and treatment of HCC, it is difficult to collect enough surgical specimens for WB analysis of GNMT expression. We tried to analyze the expression of GNMT in one pair of tumor and nontumorous specimens by using WB with mAb 14-1 and found significantly decreased levels of GNMT expression in the tumor tissue (data not shown). In this study, we used two different sets of HCC tumor and nontumorous tissue blocks, fixed in paraffin for IHC analysis. There were higher rates of detection of GNMT in the nontumorous tissues (38.5% for mAb 14-1 and 61.5% for mAb 4-17) than in the tumor tissues (0% for mAb 14-1 and 6.3% for mAb 4-17). Since different sets of tissue slides were used for the IHC assay, it was difficult to compare the sensitivities in detecting GNMT between these two mAbs. However, when paired samples were analyzed, a tendency of losing GNMT expression in both the nontumorous and tumor tissues (56.3% of the paired samples all lost GNMT expression) was demonstrated and among them, 7 pairs still exhibited at least one part of tissues with GNMT staining; it was always the tumor tissues that lost GNMT expression. Previously, using Northern blot analysis, we demonstrated that among 7 pairs of tumor and nontumorous tissues from HCC patients, 5 had diminished GNMT mRNA in the tumor tissues [9]. Recently, Avila et al. [3] reported that when compared to the normal livers, the GNMT mRNA was significantly reduced in liver cirrhosis Therefore, the downregulation of GNMT may be an early event in liver tumorigenesis. Further IHC studies with mAbs 14-1 and 4-17 on sequential samples from cirrhosis and HCC patients may elucidate the significance of the downregulation of GNMT expression in the pathogenesis of HCC.

Acknowledgements

We would like to thank Dr. W.-J. Syu and Mr. Chien-Chang Huang from the Phage Display Laboratory of the Core facilities of the National Yang-Ming University for help in the epitope mapping; Drs. Chin-Wen Chi and Anna Fen-Yau Li from the Molecular Pathology Laboratory of the Core facilities of the National Yang-Ming University for their help in the tissue staining and interpretation, and Mr. Alexander J. Boyd for help in editing the manuscript. This study was partially supported by a grant (Program for Promoting Academic Excellence, Grant No. 89-B-FA22-2-4) from the Ministry of Education, and a grant (GM 003) from the National Research Program for Genomic Medicine, Taiwan, Republic of China.

References

1 Aden DP, Fogel H, Plotkin S, Damjanov I, Knowles BB. Controlled synthesis of HbsAg in a differentiated human liver-carcinoma-derived cell line. Nature 282:615–616;1979.
2 Aida K, Tawata M, Negishi M, Onaya T. Mouse glycine N-methyltransferase is sexually dimorphic and regulated by growth hormone. Horm Metab Res 29:646–649;1997.
3 Avila MA, Berasain C, Torres L, Martin-Duce A, Corrales FJ, Yang H, Prieto J, Lu SC, Caballeria J, Rodes J, Mato JM. Reduced mRNA abundance of the main enzymes involved in methionine metabolism in human liver cirrhosis and hepatocellular carcinoma. J Hepatol 33: 907–14;2000.
4 Bhat R, Wagner C, Bresnick E. The homodimeric form of glycine N-methyltransferase acts as a polycyclic aromatic hydrocarbon-binding receptor. Biochemistry 36:9906–10;1997.
5 Bork P, Ouzounis C, Sander C, Scharf M, Schneider R, Sonnhammer E. Comprehensive sequence analysis of the 182 predicted open reading frames of yeast chromosome III. Protein Sci 1:1677–1690;1992.
6 Chang C, Lin Y, O-Lee T, Chou C, Lee T, Liu T, P'Eng F, Chen T, Hu C. Induction of plasma protein secretion in a newly established human hepatoma cell line. Mol Cell Biol 3:1133–1137; 1983.
7 Chen SY, Wong FH, Lin JR, Liu TY, Lin CH, Lin PP, Hsieh JT, Chen YM. Functional characterization of a putative tumor susceptibility gene-GNMT in the benzo[a]pyrene-detoxification pathway, submitted.
8 Chen YM, Hu CP, Chen PH, Chu MH, Tsai YT, Lee SD, Chang CM. Nuclear antigens reacted with sera and ascites of hepatocellular carcinoma patients. Hepatology 8:547–552; 1988.
9 Chen YM, Shiu JY, Tzeng SJ, Shih LS, Chen YJ, Lui WY, Chen PH. Characterization of glycine-N-methyltransferase-gene expression in human hepatocellular carcinoma. Int J Cancer 75:787–793;1998.
10 Chen YM, Chen LY, Wong FH, Lee CM, Chang TJ, Yang-Feng TL. Genomic structure, expression, and chromosomal localization of the human Glycine N-methyltransferase gene. Genomics 66:43–47;2000.
11 Chen YM, Zhang XQ, Dahl CE, Samuel KP, Schooley RT, Essex M, Papas TS. Delineation of type-specific regions on the envelope glycoproteins of human T cell leukemia viruses. J Immunol 147:2368–2376;1991.
12 Chu TM, Kawinsky E, Lin TH. Characterization of a new monoclonal antibody F4 detecting cells surface epitope and P-glycoprotein in drug-resistant human tumor cell lines. Hybridoma 12:417–429;1993.
13 Cook RJ, Wagner C. Glycine N-methyltransferase is a folate binding protein of rat liver cytosol. Proc Natl Acad Sci USA 81:3631–3634;1984.
14 Cortese R, Monaci P, Luzzago A, Santini C, Bartoli F, Cortese I, Fortugno P, Galfre G, Nicosia A, Felici F. Selection of biologically active peptides by phage display of random peptide libraries. Curr Opin Biotech 7:616–621;1996.
15 Fogh J, Trempe G. New human tumor cell line. In: Fogh J, ed. Human Tumor Cell in vitro. New York, Plenum, 115–119;1976.
16 Fogh J, Wright WC, Loveless JD. Absence of HeLa-cell contamination in 169 cell lines derived from human tumors. J Natl Cancer Inst 41:209–214;1977.
17 Fu Z, Hu Y, Konishi K, Takata Y, Ogawa H, Gomi T, Fujioka M, Takusagawa F. Crystal structure of glycine N-methyltransferase from rat liver. Biochemistry 35:11985–93;1996.
18 George JT, French RR, Glennie MJ. Measurement of kinetic binding constants of a panel of anti-saporin antibodies using a resonant mirror biosensor. J Immunol Methods 183:51–63; 1995.
19 Guan KL, Dixon JE. Eukaryotic proteins expressed in *Escherichia coli:* An improved thrombin cleavage and purification procedure of fusion proteins with glutathione S-transferase. Analyt Biochem 192:262–267;1991.
20 Heady JE, Kerr SJ. Alteration of glycine N-methyltransferase activity in fetal, adult, and tumor tissues. Cancer Res 35:640–3;1975.
21 Houser WH, Hines RN, Bresnick E. Implication of the '4S' polycyclic aromatic hydrocarbon binding protein in the trans-regulation of rat cytochrome P-450c expression. Biochemistry 24:7839–7845;1985.
22 Javitt NB. Hep-G2 cells as a resource for metabolic studies: Lipoprotein, cholesterol, and bile acids. FASEB J 4:161–168;1990.
23 Kerr SJ. Competing methyltransferase system. J Biol Chem 247:4248–4252;1972.
24 Krupenko NI, Wagner C. Transport of rat liver glycine N-methyltransferase into rat liver nuclei. J Biol Chem 272:27140–27146;1997.
25 Lai MC, Yang DR, Chuang MJ. Regulatory factors associated with synthesis of the osmolyte glycine betaine in the halophilic methanoarchaeon *Methanohalophilus portucalensis.* Appl Environ Microbiol 65:828–33;1999.
26 Lai MC, Yang DR, Chuang MJ. Activity and purification of glycine N-methyltransferase in the halophilic methanoarchaeon *Methanohalophilus portucalensis* (abstract I17) Annu Meet Am Soc Microbiol, Washington 1999.
27 Luka Z, Cerone R, III Phillips JA, Mudd HS, Wagner C. Mutations in human glycine N-methyltransferase give insights into its role in methionine metabolism. Hum Genet 110:68–74;2002.
28 MacNab GM, Alexander JJ, Lecatsas G, Bey EM, Urbanowicz JM. Hepatitis B surface antigen produced by a human hepatoma cell line. Br J Cancer. 34:509–515;1976.
29 Morgan CL, Newman DJ, Burrin JM, Price CP. The matrix effect on the kinetic rate constants of antibody-antigen interactions reflect solvent viscosity. J Immunol Methods 217:51–60;1998.
30 Mudd SH, Cerone R, Schiaffino MC, Fantasia AR, Minniti G, Caruso U, Lorini R, Watkins D, Matiaszuk N, Rosenblatt DS, Schwahn B, Rozen R, LeGros L, Kotb M, Capdevila A, Luka Z, Finkelstein JD, Tangerman A, Stabler SP, Allen RH, Wagner C. Glycine N-methyltransferase deficiency: A novel inborn error causing persistent isolated hypermethioninaemia. J Inherit Metab Dis 24:448–64;2001.
31 Nakabayashi H, Taketa K, Miyano K, Yamane T, Sato J. Growth of human hepatoma cell lines with differentiated functions in chemical medium. Cancer Res 42:3858–3862;1982.
32 Ogawa H, Fujioka M. Purification and properties of glycine N-methyltransferase from rat liver. J Biol Chem 257:3447–3452;1982.
33 Ogawa H, Gom T, Fujioka M. Mammalian glycine N-methyltransferases. Comparative kinetic and structural properties of the enzymes from human, rat, rabbit and pig livers. Comp Biochem Phys B 106:601–611;1993.
34 Ogawa H, Gomi T, Takusagawa F, Fujioka M. Structure, function and physiological role of glycine N-methyltransferase. Int J Biochem Cell B 30:13–26;1998.
35 Raha A, Wagner C, MacDonald RG, Bresnick E. Rat liver cytosolic 4 S polycyclic aromatic hydrocarbon-binding protein is glycine N-methyltransferase. J Biol Chem 269:5750–5756;1994.
36 Steward MW, Steensgaard J. Antibody Affinity: Thermodynamic Aspects and Biological Significance. In: chapter 2 The experimental determination of antibody affinity. Boca Raton, CRC Press, 65–69;1983.
37 Tseng TL, Shih YP, Huang YC, Wang CK, Chen PH, Chang JG, Yeh KT, Chen YM, Buetow KH. Genotypic and phenotypic characterization of a putative tumor susceptibility gene, *GNMT* in liver cancer. Cancer Res, in press.